Detection and Imaging in Complex Media with the D.O.R.T. Method

Claire Prada

Laboratoire Ondes et Acoustique, ESPCI
10 rue Vauquelin, 75231 Paris, Cedex 05, France
claire.prada-julia@espci.fr

Abstract. Acoustic waves are used for detection, localization and sometimes destruction of passive targets. In most fields of acoustics, arrays of transmitters and arrays of receivers are available, and if not synthetic aperture techniques can be used. With such arrays, a great amount of data can be collected, and the general problem is to extract the relevant information from these data to detect (or to form an image of) a scattering object. This problem appears in applications ranging from medical imaging to underwater acoustics and even in seismology. The D.O.R.T. method is a new approach to active detection and focusing of acoustic waves using arrays of transmitters and receivers. This method was derived from the theoretical study of iterative time-reversal mirrors. It consists essentially of the construction of the invariants in the time-reversal process. After explaining the basic theory of the D.O.R.T. method, several experimental results are shown: (a) detection and selective focusing through an inhomogeneous medium; (b) detection and focusing in a water waveguide, where high resolution is achieved by taking advantage of the multiple paths in the guide; (c) an analysis of scattering by a thin hollow cylinder, where the various components of the elastic waves circumnavigating in the shell are separated; and (d) in some cases the eigenvectors obtained at different frequencies can be combined to obtain the time-domain Green's function of each scatterer.

1 Introduction

In various domains, such as medicine, nondestructive evaluation (NDE), underwater science and seismology, acoustic waves are used for detection, localization and sometimes destruction of passive targets. In most fields of acoustics, arrays of transmitters and arrays of receivers are available, and if not synthetic aperture techniques can be used.

The D.O.R.T. method provides a new approach to active detection and focusing of acoustic waves using an array of transmitters and an array of receivers. It is an analysis technique of pulse–echo measurements (or reflection data) that may be interesting for applications ranging from medical imaging, where arrays of transmit-receive transducers are currently used, to underwater acoustics and even seismology, where an ensemble of seisms can be considered as an array of transmitters and an ensemble of stations as an array of receivers.

With multiple sources and multiple receivers, a large amount of scattering data can be collected which correspond to different acoustic paths in the medium under study. The general problem is to extract the relevant information from these data to detect (or to form an image of) a scattering object in the medium.

For typical length scales, the low velocity of acoustic waves allows information coming from different parts of the studied medium to be separated. However, the detection sensitivity as well as the quality of the image of scattering objects depend on the ability to focus energy in the medium either in transmission or in reception. This focusing is also crucial for destruction techniques like lithotripsy. The presence of an aberrating medium between the object and the arrays can detrimentally alter the beam profiles.

In NDE, cracks and defects can be found within materials of various shapes. The samples to be evaluated are usually immersed in a pool, and the interface shape between the samples and the coupling liquid currently limits the detectability of small defects. In medical imaging, one looks for organ walls, calcification, tumors, kidney or gallbladder stones. A fat layer of varying thickness, bone tissue, or some muscular tissues may greatly degrade focusing. In underwater acoustics, one looks for mines, submarines, or objects buried under sediments. Refraction by the oceanic structure ranging in scale from centimeters to tens of kilometers is an important source of distortions. In seismology, detection of discontinuities such as local changes in reflectivity at the core–mantle interface can be achieved by inversion of reflection data. However, the poor knowledge of the acoustic properties of the medium renders this problem rather difficult.

During the past 10 years, *Fink* and his team have developed time-reversal techniques in order to achieve optimum focusing through distorting media (this volume) [1,2]. They have shown through several ultrasonic experiments that high-quality focusing can be obtained with acoustic time-reversal mirrors. In echographic mode, this self-focusing technique is effective in the presence of a single scatterer in the medium. When this medium contains several scattering centers, the time-reversal operation need to be iterated in order to select one of them. In general, after some iterations, the process converges and produces a wave front that focuses on the most reflective scatterer [3].

In some situations, it is interesting to learn how to focus on weaker scattering centers. The D.O.R.T. method provides a solution to this problem [4,5,6]. This method was derived from the theoretical study of iterative time-reversal mirrors and consists essentially of the construction of the signal patterns that are invariants under a time-reversal process. Those invariants appear as the eigenvectors of a matrix called the time-reversal operator which describes the time-reversal process. The eigenvectors are calculated offline after the measurement of the response function of the array in the presence of the scattering medium. It is not a real-time procedure; however, it can still be applied in many experimental situations. The D.O.R.T. method shares some

of the principles of eigenvector decomposition techniques that are used in passive source detection [7,8,9]. However the latter assume statistically uncorrelated sources, while the D.O.R.T. method is active and deterministic; thus they should not be considered as competing techniques.

The basic theory of the D.O.R.T. method is explained in Sect. 2; experimental illustrations follow. An example of detection and selective focusing through an inhomogeneous medium is shown in Sect. 3. Examples of detection and focusing in a water waveguide are presented in Sect. 4. The method can also take advantage of the matched-filter property of the waveguide in order to separate the echoes from different scatterers with high resolution.

Sect. 5 is devoted to the analysis of the scattering by a thin hollow cylinder. It is shown how the D.O.R.T. method separates the various components of the elastic waves circumnavigating in the shell. In Sects. 3 to 5 the pulse-echo measurements are analysed frequency by frequency. In general, it is not possible to get back to the time domain; however, in Sect. 6, we show that in some cases the eigenvectors obtained in the whole frequency band of the transducers can be combined to obtain the time-domain Green's function of each scatterer.

2   Basic Principle of the D.O.R.T. Method

The D.O.R.T. method has been presented in several papers [4,5,6]. It consists of determining the transmitted waveforms that are invariant under the time-reversal process. We show that for a set of well-resolved scatterers the focusing on one of them is invariant in this manner. The analysis is based on a matrix formalism that describes the transmit–receive process. To begin, we introduce the transfer matrix of the system and the corresponding time-reversal operator.

2.1   The Transfer Matrix

An array of N transmitters (array No. 1) insonifying a scattering medium and an array of receivers (array No. 2) are considered. This system is assumed to be a linear and time-invariant system of N inputs and L outputs. Thus it is characterized by $N \times L$ inter-element impulse response functions. Let $h_{lm}(t)$ be the signal delivered by receiver l when a temporal delta function $\delta(t)$ is applied on the transmitter number m. These $N \times L$ functions provide a complete description of the transmit–receive process. Indeed, if $e_m(t), 1 < m < N$ are the transmitted signals, then the received signals are given by the equation

$$r_l(t) = \sum_{m=1}^{N} k_{lm}(t) \underset{t}{\otimes} e_m(t). \tag{1}$$

These L equations simplify in the frequency domain in a matrix form: any transmit–receive operation is described with a complex transfer $L \times N$ matrix $\mathbf{K}(\omega)$ by the equation:

$$\boldsymbol{R}(\omega) = \mathbf{K}(\omega)\boldsymbol{E}(\omega)\,, \tag{2}$$

where ω is the frequency, $\boldsymbol{E}(\omega)$ is the transmitted vector of N components, $\boldsymbol{R}(\omega)$ is the received vector of L components and $\mathbf{K}(\omega)$ is the $L \times N$ transfer matrix of the system.

2.2   Invariants of the Time-Reversal Process and Decomposition of the Transfer Matrix

In most time-reversal experiments shown by Fink and his team, a single array is used in both transmit and receive modes. In the case where the transmitter and the receiver arrays are distinct, the time-reversal experiment can only be an hypothetical experiment: one can imagine a time-reversal operation between the two arrays, assuming that array No. 1 becomes the receiver and array No. 2 becomes the transmitter. Neglecting the impulse responses of the transmitter and receivers, the reciprocity principle guaranties that the response from element number l of array No. 2 to element number n of array No. 1 is equal to the response from element number n to element number m. Consequently, the transfer matrix from array No. 2 to array No. 1 is $^{t}\mathbf{K}(\omega)$.

A time-reversal operation $t \rightarrow -t$ is equivalent to a phase conjugation in the frequency domain. Thus, in a time-reversal process, if $\boldsymbol{E}_0(\omega)$ is the first transmitted signal (applied on array No. 1) of a time-reversal process, then the second transmitted signal (applied on array No. 2) is the phase conjugate of the received signal:

$$\boldsymbol{E}_2(\omega) = \mathbf{K}^{*}(\omega)\boldsymbol{E}_1^{*}(\omega)\,. \tag{3}$$

After transmission of $E_2(\omega)$, the signal received on array No. 1 is

$$\boldsymbol{R}(\omega) = {}^{t}\mathbf{K}(\omega)\mathbf{K}^{*}(\omega)\boldsymbol{E}_1^{*}(\omega)\,. \tag{4}$$

This signal is linked to the first transmitted signal through a phase conjugation, and the product by the matrix $^{t}\mathbf{K}^{*}(\omega)\mathbf{K}(\omega)$. Thus, this matrix allows any time-reversal process to be described and is called the time-reversal operator. Note that this approach is more general than the one presented in [4,5]. Indeed, in these papers, the same array acts as transmitter and receiver. In this case, the reciprocity principle insures that the transfer matrix $\mathbf{K}$ is symmetrical and the time reversal operator is simply $\mathbf{K}^{*}(\omega)\mathbf{K}(\omega)$. In the experiments that will be shown in the following sections, a single array is used. However, the theory presented here as well as in [6] is more general and broadens the field of application of the D.O.R.T. method. The important property of the time-reversal operator is that it is hermitic with positive eigenvalues.

Let the first transmitted signal be $V(\omega)$, an eigenvector of $^t K^*(\omega) K(\omega)$ associated to the eigenvalue $\lambda(\omega)$, then after a time-reversal process the received signal is $\lambda(\omega) V^*(\omega)$, which is proportional to the conjugate of $V(\omega)$. Consequently one can say that the eigenvectors of $^t K^*(\omega) K(\omega)$ correspond to waveforms that are invariants of the time-reversal process.

In fact, from a mathematical point of view, the diagonalization of $^t K^*(\omega) K(\omega)$ is equivalent to the singular value decomposition (SVD) of the transfer matrix $K(\omega)$. Indeed, the SVD is $K(\omega) = U(\omega) \Lambda(\omega) V^+(\omega)$, where $\Lambda(\omega)$ is a real diagonal matrix of the singular values and $U(\omega)$ and $V(\omega)$ are unitary matrices. The eigenvalues of $^t K^*(\omega) K(\omega)$ are the squares of the singular values of $K(\omega)$; its eigenvectors are the columns of $V(\omega)$. We shall use this decomposition in the following. Note that when a column of $V(\omega)$ is transmitted on the first array, the signal received on the second array is proportional to a column of $U(\omega)$.

2.3 Transfer Matrix for Point-Like Scatterers

In the case of point-like scatterers the transfer matrix can be derived easily. We assume that the medium contains d point-like (Rayleigh) scatterers with complex frequency-dependent reflectivity coefficients $C_1(\omega), C_2(\omega), \ldots, C_d(\omega)$. Then the transfer matrix can be written as the product of three matrices: (a) a propagation matrix that describes the transmission and the propagation from the transducers to the scatterers, (b) a scattering matrix which is diagonal in the case of a single scattering process, and (c) the back propagation matrix.

Let $h_{1,il}(t)$ be the diffraction impulse response function of the transducer number l of array 1 to the scatterer number i with Fourier transform $H_{1,il}(\omega)$. Let $a_e(t)$ and $a_r(t)$ be the transducer acousto-electrical response in emission and in reception, with Fourier transforms $A_e(\omega)$ and $A_r(\omega)$. If the input signal at each element l is $e_l(t)$, then the pressure at the scatterer i is

$$p_i(t) = \sum_{l=1}^{N} h_{1,il}(t) \underset{t}{\otimes} a_e(t) \underset{t}{\otimes} e_l(t). \tag{5}$$

This equation is written in the frequency domain as

$$P_i = A_e \sum_{l=1}^{N} H_{1,il} E_l. \tag{6}$$

The expression is simplified using matrix notation:

$$P = A_e H_1 E, \tag{7}$$

where E is the input vector signal, P is the vector representing the pressure received by the d scatterers and H_1 is a matrix of dimensions $N \times d$ called the diffraction matrix.

In the case of single scattering, the pressure reflected by scatterer number i is $C_i P_i$. Therefore, the vector of reflected pressures is the matrix $\mathbf{C}P$ where $\mathbf{C}$ is a diagonal matrix of coefficients $C_{ij} = \delta_{ij} C_i$ for all i, j in $1, \ldots, d$.

According to the reciprocity principle, the propagation from the scatterer number i to the transducer number n of array 2 is $h_{2,in}(t)$, so that the back-propagation matrix is the transpose of the propagation matrix ${}^t\mathbf{H}_2$. Consequently, the output signal R at array number 2 is

$$R = A_e A_r^t \mathbf{H}_2 \mathbf{C} \mathbf{H}_1 E \tag{8}$$

The expression of the transfer matrix is then

$$\mathbf{K} = A_e A_r^t \mathbf{H}_2 \mathbf{C} \mathbf{H}_1 . \tag{9}$$

2.4   Decomposition of K for Well-Resolved Scatterers

The iterative time-reversal process allows selective focusing on the most reflective of a set of scatterers. In some cases it might be interesting to learn how to focus on the other scatterers. For example, this is the case in lithotripsy when several lithiases exist. The theoretical analysis of the iterative time-reversal process has provided a solution to this problem.

We now propose to compute the SVD of the transfer matrix in a scattering medium containing D point-like scatterers. According to Sect. 2.3, if $\mathbf{H}_1$ ($\mathbf{H}_2$) is the matrix of size $D \times N$ ($D \times L$) that describes the propagation from array No. 1 (array No. 2) to the D scatterers and $\mathbf{C}$ the diagonal matrix of size $D \times D$ that describes single scattering, and if the responses of the transmitter and receivers are assumed to be temporal delta functions, then

$$\mathbf{K} = {}^t\mathbf{H}_2 \mathbf{C} \mathbf{H}_1 . \tag{10}$$

We can say that the targets are ideally resolved if the time-reversal focusing on one of them does not produce energy on the others. From a mathematical point of view, it means that the columns of the propagation matrix $\mathbf{H}_i$ are orthogonal. If this property is satisfied for both arrays and if the "apparent reflectivities" (this phrase will be discussed further) of each target are different, the eigenvectors of the time-reversal operator can be analytically determined. We note that $\overline{\mathbf{H}_i} i = (1, 2)$ is the matrix whose rows are the normalized rows of $\mathbf{H}_i$. We can then write $\mathbf{H}_i = \Delta_i \overline{\mathbf{H}_i}$ where Δ_i is a diagonal matrix of coefficients the norms of the column of $\mathbf{H}_i$. The following equation is deduced:

$$\mathbf{K} = {}^t\overline{\mathbf{H}_2} \Delta_2 \mathbf{C} \Delta_1 \overline{\mathbf{H}_1} \tag{11}$$

This decomposition is the SVD of $\mathbf{K}$. Indeed, as $\overline{\mathbf{H}_i} i = (1, 2)$ are normalized, they satisfy the equations ${}^t\overline{\mathbf{H}_1} \overline{\mathbf{H}_1^*} = I$ and ${}^t\overline{\mathbf{H}_2} \overline{\mathbf{H}_2^*} = I$; they are unitary matrices.

The matrix $\Delta_2 C \Delta_1$ is real diagonal, with terms equal to

$$\lambda_i = C_i \sqrt{\sum_{n=1}^{N} |H_{1,in}|^2} \sqrt{\sum_{n=1}^{N} |H_{2,in}|^2} \quad \text{for} \quad 1 < i < D. \tag{12}$$

λ_i is precisely what we call the apparent reflectivity of scatterer number i. It is proportional to its reflectivity C_i and to a term that depends on the diffraction pattern of both the transmitter and receiver arrays.

Consequently, the eigenvectors of ${}^t\mathbf{K}^*\mathbf{K}$ are the complex conjugate of the first columns of $\overline{\mathbf{H_1}}$:

$$\frac{H_{1,i}^*}{\sqrt{\sum_{n=1}^{N} |H_{1,in}|^2}} \quad \text{for } 1 < i < D. \tag{13}$$

According to the reciprocity theorem, each of them is precisely the time-reversed form of the signal that would be received on array No. 1 if target number i was acting as a point-like acoustic source.

Finally, for well-resolved point-like scatterers the number of nonzero eigenvalues is equal to the number of scatterers. Furthermore, if the scatterers have different apparent reflectivities (λ_i), each eigenvector is associated with one scatterer; the phase and amplitude of the eigenvector should be applied to each transducer in the array in order to focus on that particular scatterer.

If the scatterers have equal apparent reflectivities, or are not resolved, the problem is more complicated and beyond the scope of this paper. However, some results in this regard can be found in [5].

2.5   The D.O.R.T. Method in Practice

The first step is the measurement of the inter-element impulse responses of the system. Since the reception system operates in parallel, this measurement requires N transmit–receive operations for an array of N transducers. The first transducer of the array is excited with a signal $e(t)$, and the signals received on the N channels are stored. This operation is repeated for all the transducers of the array with the same transmitted signal $e(t)$. The components of the transfer matrix $\mathbf{K}(\omega)$ are obtained by a Fourier transform of each signal. This measurement could also be done with any multiplexed system by N^2 transmit–receive operations.

The second step is the SVD of the transfer matrix $\mathbf{K}(\omega)$ at a chosen frequency. The singular value distribution contains valuable information as the number of secondary sources in the scattering medium.

The third step is to back-propagate each eigenvector. This can be done either numerically or experimentally. This is useful to focus through an aberrating medium selectively on each scatterer.

Detection consists of the following steps: First, the inter-element impulse response functions $k_{lm}(t)$ are measured. Second, the transfer matrix is calculated at one chosen frequency (more often the central frequency of the

transducers). Last, the SVD of the transfer matrix is calculated: $\mathbf{K}(\omega) = \mathbf{U}(\omega) \Lambda(\omega) \mathbf{V}^+(\omega)$, where $\Lambda(\omega)$ is a real diagonal matrix of the singular values and $\mathbf{U}(\omega)$ and $\mathbf{V}(\omega)$ are unitary matrices.

3   Selective Focusing Through an Inhomogeneous Medium with the D.O.R.T. Method

The first application of this method is to learn how to focus selectively through an inhomogeneous layer. A simple example is now presented. A single linear array of 128 transducers is used for transmission and reception. The array pitch is 0.4 mm, and the central frequency is 3 MHz with 60% bandwidth. The sampling frequency of received signals is 20 MHz. The scatterers are two wires placed at 90 mm perpendicular to the array. A rubber layer of varying thickness is placed between the array and the wires (Fig. 1).

First, cylindrical time delay laws are applied to the transducers in order to focus on the wires as if there was no aberration. The pressure pattern is measured with a hydrophone in the plane of the wires: the layer induces severe defocusing (Fig. 2). Now the question is: how can we obtain a good focusing without any information on the acoustic properties of the layer.

The inter-element impulse response functions of all the elements of the array were measured. The responses of element 64 to the 128 elements of the array are shown in Fig. 3: the wavefronts corresponding to the echo of the two wires can easily be seen.

The transfer matrix $\mathbf{K}$ was computed at the frequency of 3 MHz. Note that the Fourier transforms of the signals displayed in Fig. 3 provide column 64 of $\mathbf{K}$.

The SVD of $\mathbf{K}$ reveals 2 significant singular values among 128 (Fig. 4), which indicates the presence of two scattering centers. The phase laws of the corresponding eigenvectors (Fig. 5) are unwrapped to form time-delay laws (Fig. 6). Each time delay law is well defined and corresponds to one of the wires. To confirm this, the time-delay laws are used to focus through the
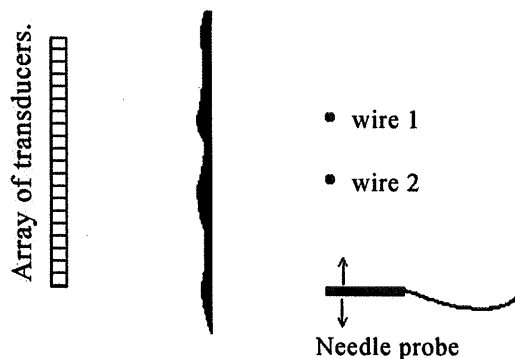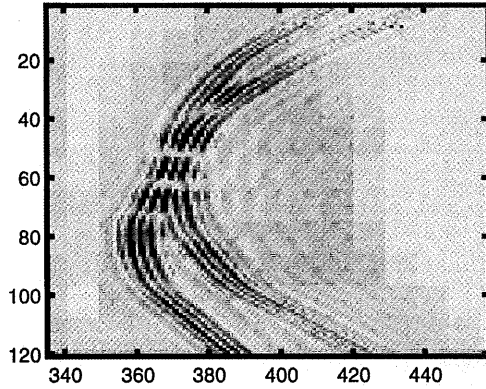

Fig. 1. Geometry of the experiment

Fig. 2. Echo of the two wires after illumination by the center element of the array (horizontal axis: time in μs, vertical axis: array element)
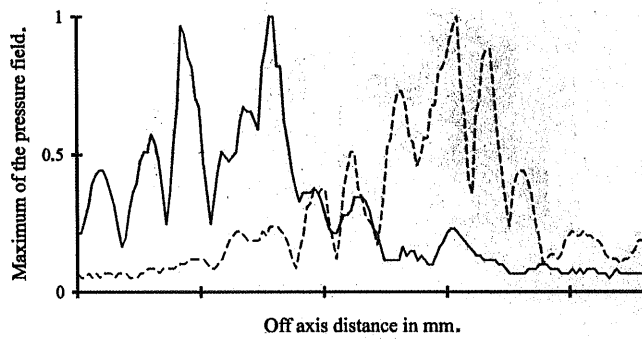

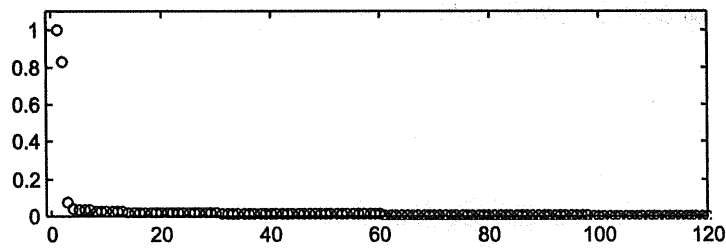**Fig. 3.** Pressure pattern obtained by cylindrical focusing through the rubber layer

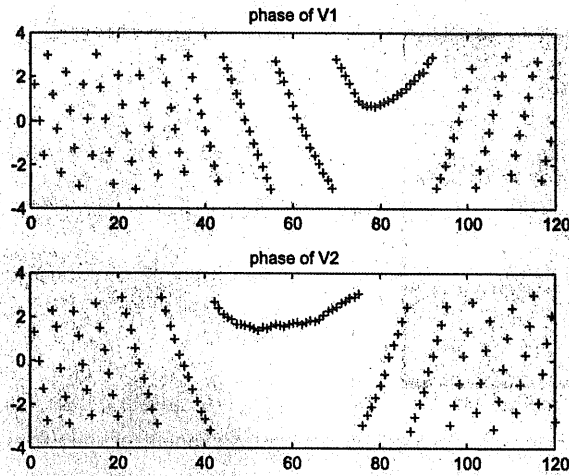**Fig. 4.** Singular values of the transfer matrix

phase of V1

phase of V2

Fig. 5. Phase laws of the first and second eigenvectors
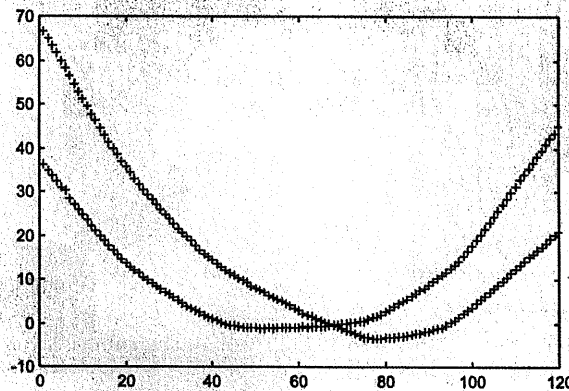
Fig. 6. Unwrapped phase laws of the first and second eigenvectors

rubber layer. The so-produced pressure field is measured in the plane of the wires (Fig. 7). Each eigenvector focuses on one of the wires and the accuracy of the focusing is similar to what can be obtained with this array in water only.

4   Highly Resolved Detection and Selective Focusing in a Waveguide

The problem of optimum signal transmission and source location in a waveguide has been the subject of many theoretical and experimental works. The propagation of an acoustic pulse inside a waveguide is a complex phenomenon. This complexity renders the detection and imaging process very difficult.
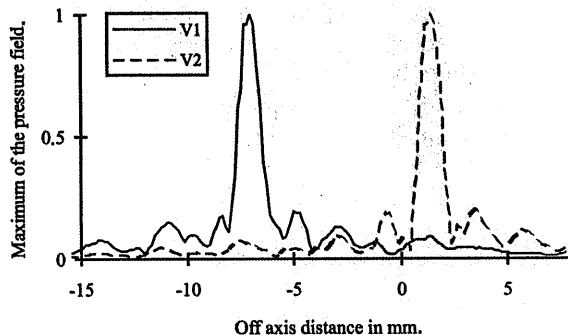
Fig. 7. Pressure patterns measured at the position of the wires after transmission of the first and second eigenvectors

Because of multiple-path effects, the Green's function that is used in matched-field processing is nontrivial, and its calculation requires accurate knowledge of the medium. However, several studies have shown how to take advantage of this complexity.

In waveguide transmission, the guide can be considered as a linear filter. *Parvulescu* et al. [10] reported a matched-filter experiment in the ocean between a source and a receiver. They recorded the reception of an impulsive transmission and replayed the time-reversed signal through the source. They obtained a high temporal compression, which was explained by the coherent recombination of the energy received over the different multiple paths. They also showed the high sensitivity to small displacements of the source, suggesting that this property should be used to locate the source. As proposed by *Clay* [11] and *Li* [12], the combination of array-matched filter and time-domain-matched signal techniques improve the accuracy in source localization. In these papers, the focusing is explained in terms of matched signal: the waveguide plays the role of a correlator.

The possibility of taking advantage of the invariance of the acoustic wave equation under time reversal in order to achieve highly resolved spatial and temporal focusing in a waveguide arose afterward. In 1991, *Jackson* et al. [13] provided a theoretical analysis of the time-reversal process in a water channel. Focusing experiments inside a water waveguide with a time-reversal mirror were made by *Roux* et al. [14]; then Kuperman and his team implemented a time-reversal mirror in the Mediterranean Sea [15,16,17]. They demonstrated how to refocus an incident acoustic field back to its origin and to achieve high temporal and spatial compression by time reversal of the wave field.

In the above-mentioned papers, only transmission from sources to receivers is considered. A natural question is how to use this super focusing property in echographic mode to detect and separate scatterers. In echographic mode, the signal reflected from a scatterer is extremely complex because it has undergone a double path through the guide. The D.O.R.T.

method was applied to this problem [18]: the separation and selective focusing on two scatterers and then the detection of a scatterer placed near an interface of the guide are shown in the following.

Finally, in a steel-water-air waveguide, the consequences of surface waves produced at the water-air interface on the performance of the D.O.R.T. method are studied.

4.1   Selective Highly Resolved Focusing in a Waveguide

The experiment is performed in a 2-dimensional water waveguide, delimited by two water–steel plane interfaces. The water layer is 35 mm thick. The array consists of 60 transducers with a central frequency of 1.5 MHz; it spans the whole height of the guide. The array pitch is equal to 0.58 mm. The scatterers are two wires of diameters 0.1 mm and 0.2 mm, spaced 2 mm, and placed perpendicular to the array axis at a distance of 400 mm (Fig. 8). As the average wavelength is 1 mm, both wires behave almost like point scatterers. For this range and this frequency, the free-space diffraction focal width is 12 mm, so the two wires are not resolved by the system.

The echographic signals recorded after a pulse is applied to one transducer of the array are very complex with a low signal-to-noise ratio. The inter-element response $k_{2840}(t)$ is a typical example (Fig. 9). After approximately 5 reflections at the interfaces the signal can no longer be distinguished from noise. The echoes of the two wires are superimposed and cannot be separated in a simple manner.

The 60×60 impulse response functions are measured, and the transfer matrix is calculated at a frequency of 1.5 MHz. The decomposition reveals two singular values that are separated from the 58 "noise" singular values (Fig. 10). The "noise" singular values are partly explained by electronic and quantification noises. However, different second-order acoustical phenomena not taken into account in the model probably contribute to these singular values; these include the defects of the interfaces, the elastic responses of the wires, the multiple echoes between the wires, and also coupling between the transducers.

The eigenvectors V_1 and V_2 have a complicated phase and amplitude distribution, and it is impossible to tell to which scatterer each of them corresponds. These distributions are applied to the array of transducers. Namely, if $\mathbf{V_1} = (A_1 e^{i\varphi_1}, A_2 e^{i\varphi_2}, \ldots, A_n e^{i\varphi_n})$ is the first eigenvector, then the signal $s_p(t) = A_p \cos(\omega t - \varphi_p)$ is applied to transducer number p. The
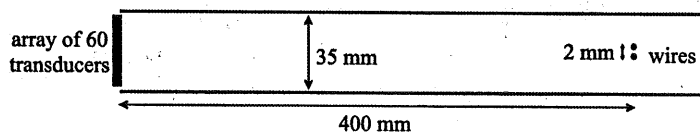
array of 60 transducers   35 mm   2 mm ⁚ wires

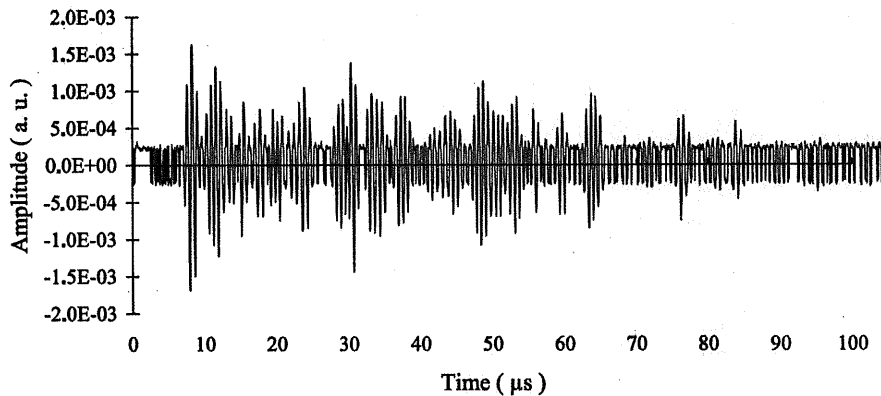← 400 mm →

Fig. 8. Geometry of the experiment

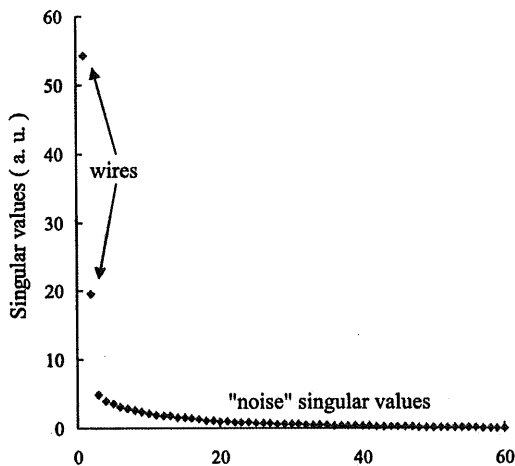**Fig. 9.** Typical echo of the wires: inter-element impulse responses $k_{2840}(t)$

Fig. 10. Singular values of the transfer matrix calculated at 1.5 MHz

so-produced pressure field is measured across the guide at the range of the wires (Fig. 11). For each eigenvector, the wave is focused at the position of one wire. In both cases the residual level is lower than $-18\,$dB and the $-6\,$dB focal width is 1.4 mm. In fact, the width is overestimated because the width of the probe is 0.5 mm; the real focal width is probably around 1.2 mm, which is 9 times thinner than the theoretical free space focal width.

For comparison, the same experiment was performed after removing the guide. In this case the wires are not resolved, and only the first singular value is significant. The pressure pattern is measured for transmission of the first eigenvector; the focal width is 13 mm (Fig. 11). Consequently, the guide allows a focusing at least 10 times thinner than in free space to be achieved.
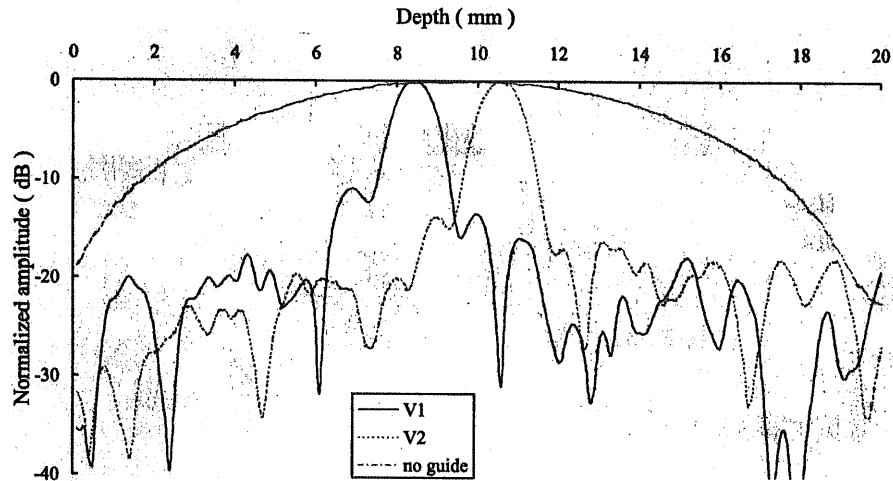
Fig. 11. Pressure pattern measured across the guide at the range of the wires after transmission of the eigenvectors. *Solid and dotted lines* first and second eigenvectors, respectively, obtained with the guide; first *gray line* eigenvector without the guide

The angular directivity of each transducer limits the number of reflections at the guide interfaces that can be recorded. This induces an apodization of the virtual array made of the set of images of the real one. Taking this phenomenon into account, the focal width roughly corresponds to a virtual aperture consisting of 8 pairs of images of the array.

4.2   Detection Near the Interface

In many cases, the detection of a defect near an interface is difficult, especially if the reflectivity coefficient of the interface is close to −1, which is the case for the water–air interface. Indeed, in this situation, the virtual image of the defect with respect to the interface behaves as a source in opposite phase to the defect. The real source and the virtual source interfere in a destructive way so that the reflected signal is very low. The ability of the D.O.R.T. method to detect a wire that is close to a water–air interface was analyzed. The experiment was done in a water waveguide of 35 mm width limited by air at the surface and steel at the bottom. A wire of 0.2-mm diameter is placed inside the guide 400 mm from the array. The wire is moved step by step from the bottom to the surface, and for each position the transfer matrix is measured and decomposed. The two first singular values are display versus distance to the surface in Fig. 12. The first singular value represents the signal level, and the second the noise level. When the wire reaches the bottom, the singular value increases rapidly by a factor of two. The echoes from the scatterer and from its image add constructively. Conversely, when the wire gets to the surface, the singular value decreases rapidly. It remains well

separated from the noise singular values until the distance between the wire and the interface reaches $\lambda/5$. This result shows that the distance under which the scatterer is no longer detectable is less than $\lambda/5$ at a range of 400λ.
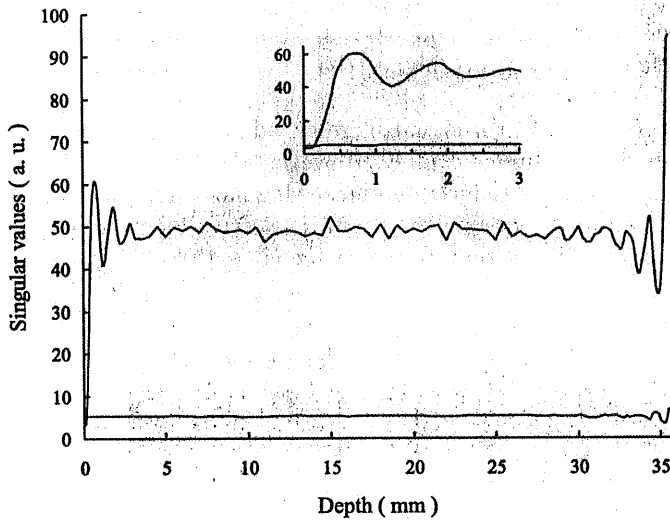

Fig. 12. Dependence of the singular values of the transfer matrix on the distance to the surface

4.3 Detection in a Nonstationary Waveguide

The efficiency of the method in a nonstationary guide with surface waves at the water-air interface is now studied. A vertical plate with horizontal oscillations at 6 Hz produces surface waves with a typical wavelength of 30 mm. The height of the waves is varied using a diaphragm (Fig. 13). The root-mean-square (rms) height of the waves kh_{rms} is varied from 0 to 1.7 mm,
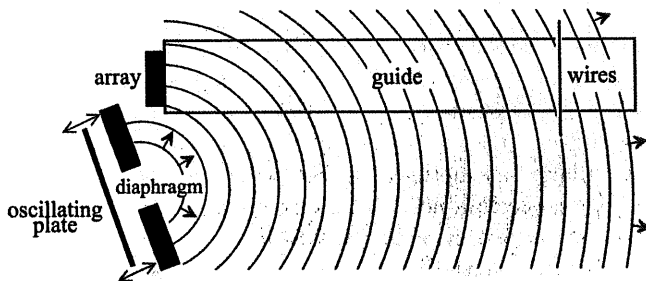

Fig. 13. Experimental setup to produce surface waves

which corresponds to $0 < kh_{rms} < 10$. The array of transducers is the same as before. Two wires are placed 500 mm from the array and spaced 5 mm.

For each value of kh_{rms}, the transfer matrix is measured and decomposed. While kh_{rms} is lower than 1.5, the two higher singular values are well separated from noise singular values. The corresponding eigenvectors focus at the position of the wires; however, the main lobes are approximately 1.6 times larger and the residual lever 2 times higher than in the absence of waves (Fig. 14).

For high waves ($kh_{rms} = 10$), the signal singular values are not separated from noise with a single measurement of K. However, the average of 10 realizations of the transfer matrix reduces the noise singular values enough to separate the wires. Then it is possible to obtain a selective focusing with a resolution almost 3 times thinner than in free space (Fig. 15).
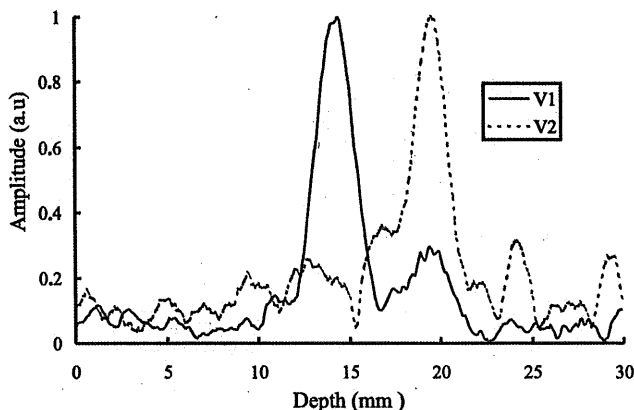

Fig. 14. Pressure field measured for transmission of eigenvectors 1 and 2 calculated with an unaveraged transfer matrix obtained with surface waves of $h_{rms} = 0.23$ mm

5   Inverse-Scattering Analysis and Target Resonance

The preceding experiments illustrate the efficiency of the D.O.R.T. method to focus selectively on different scatterers through complex media. More generally this method isolates and classifies the scattering centers or secondary sources in the medium and can be used to analyse the scattering from extended objects. In particular, this method applies to scattering by a thin hollow cylinder. Time-reversal techniques with short ultrasonic signals have been applied to such scattering experiment by *Thomas* et al. [9]. They are efficient when the contributions of the various waves can be selected by a time window. It is now shown that even if the waves interfere in time it is possible to separate them using the D.O.R.T. method [20,21].
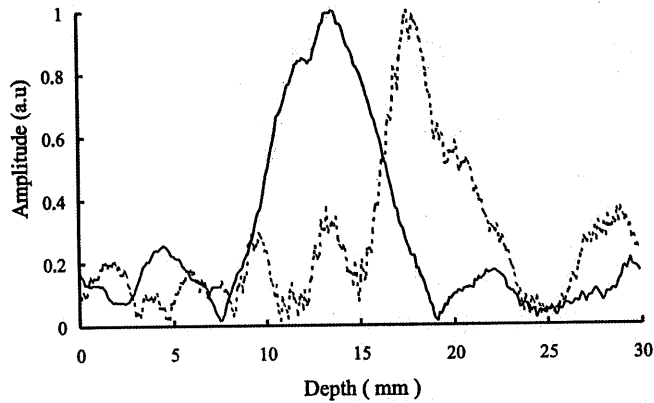
Fig. 15. Pressure field measured for transmission of eigenvectors 1 and 2 calculated from an average of ten realizations of the transfer matrix

5.1 Experiment

The array is linear and made of 96 rectangular transducers similar to those used in Sect. 3. A hollow steel cylinder with a diameter of 20 mm and a thickness of approximately 0.6 mm is placed perpendicular to the array of transducers at a distance of 80 mm symmetrically with respect to the array axis (Fig. 16). For an incident plane wave, a Lamb wave is generated at a given angle of incidence, θ, with respect to the normal to the surface. This angle satisfies the relation $\sin(\theta) = \frac{C_0}{C_\phi}$, where C_0 is the sound velocity in water and C_ϕ is the phase velocity of the Lamb wave.

Consequently, two Lamb waves are generated at points A and B, symmetrical with respect to the incident direction (Fig. 17). While propagating around the cylinder, those two waves radiate backward from the same points, A and B, which behave as secondary sources. The distance d_{AB} between those
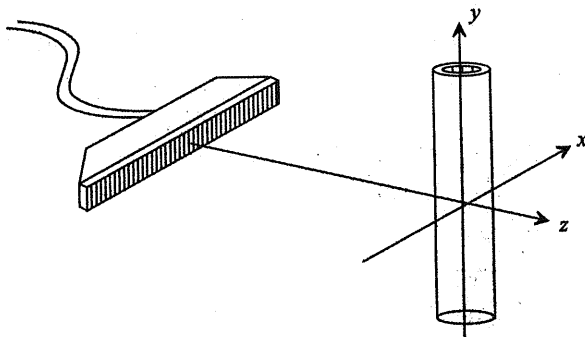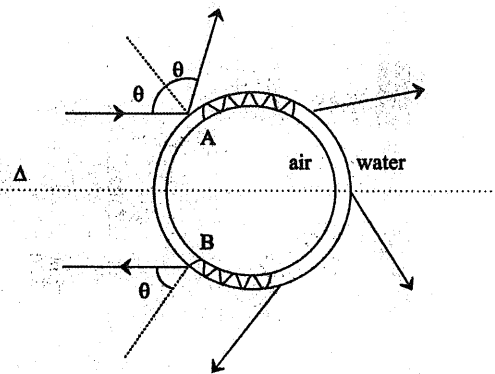

Fig. 16. Experimental setup

Fig. 17. Generation and radiation of a Lamb wave on a thin hollow cylinder

points is given by

$$d_{\mathrm{AB}} = D \frac{C_0}{C_\phi}, \tag{14}$$

where D is the diameter of the cylinder. Thus, the nature of the wave can be determined by knowing its radiation points. For such a thickness and frequency range, the dispersion curves (Fig. 18) predict that radiation of the three Lamb waves A_0, S_0 and A_1 should be observed.

A short pulse is launched from the center element of the array. The echo of the cylinder is recorded on the 96 elements (Fig. 19). The first wavefront corresponds to the strong specular echo. The signal observed later is the elastic part of the echo. Between 15 ms and 25 ms, two pairs of wavefronts with interference fringes can be distinguished. Those wavefronts correspond to the radiation of two pairs of circumferential waves after one turn around
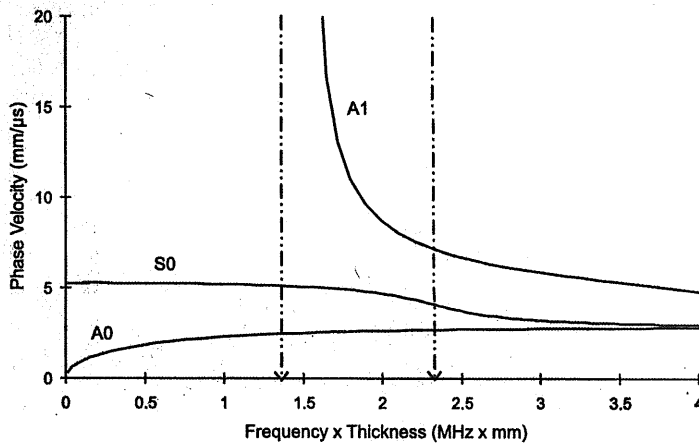

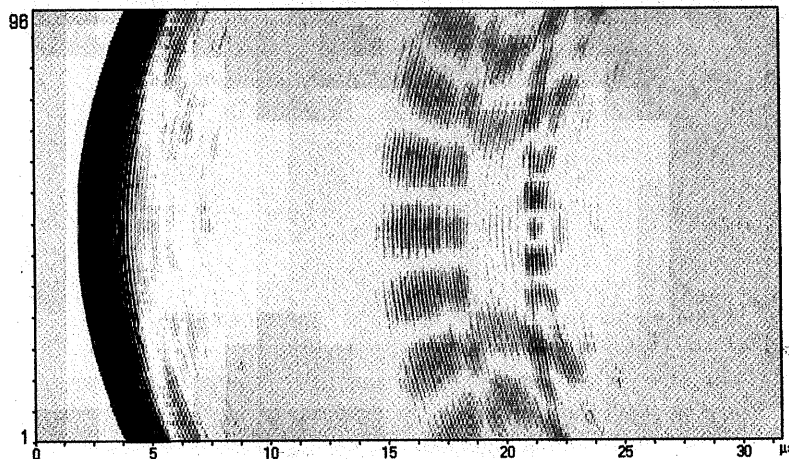**Fig. 18.** Dispersion curves of Lamb waves for a steel plate

Fig. 19. Echo of the shell received by the 128 transducers after transmission of a short pulse from the center element of the array. The first wavefront is the specular echo, the second the contribution of the S_0 Lamb wave and the third the contribution of the A_0 Lamb wave

the shell. The first one is identified as the S_0 Lamb mode, and the second as the A_0 Lamb mode. Interfering with those well-defined wavefronts is the contribution of the highly dispersive A_1 wave.

5.2   Invariants of the Time-Reversal Process

The two circumferential waves generated at points A and B (Fig. 17) are linked by reciprocity. The first one can be obtained by time reversal of the second one. Both waves are invariant under two successive time-reversal processes; consequently they should be associated to eigenvectors of the time-reversal operator. In fact, due to the symmetry of the problem, they are both associated with the same two eigenvectors: one corresponding to the generation in phase with the two waves, and the other to the generation in opposite phase.

To separate these contributions we now apply the D.O.R.T. method. After the measurement of the 96×96 inter-element impulse responses, the whole process remains numerical. Only the elastic part of the signal is used to calculate the time-reversal operator (between 15 ms and 25 ms). At 3.05 MHz, the diagonalization of the time-reversal operator has six dominant eigenvalues. The modulus of the components of each eigenvector (1 to 6) is represented versus array element in Fig. 20. The interference fringes are easily observed. They are the equivalent at one frequency of the interference pattern observed on the echoes. As in the experiment with two wires (1.4), this means that an eigenvector corresponds to the interference of two coherent point sources.
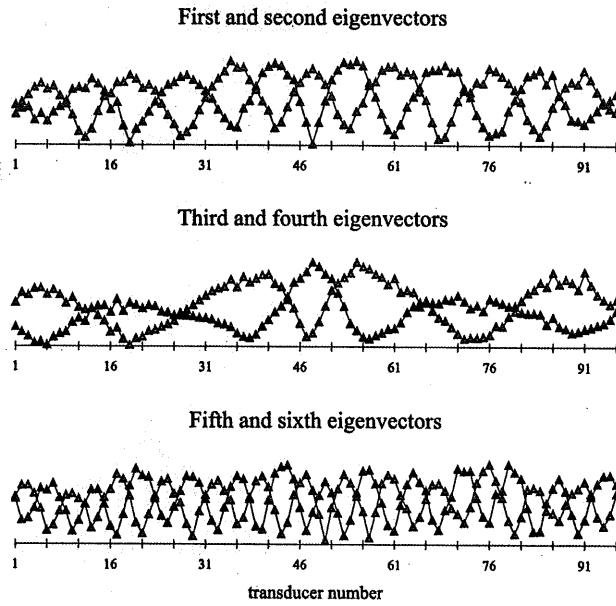
First and second eigenvectors

1   16   31   46   61   76   91

Third and fourth eigenvectors

1   16   31   46   61   76   91

Fifth and sixth eigenvectors

1   16   31   46   61   76   91

transducer number

Fig. 20. Modulus of the components of the 6 eigenvectors

The numerical back-propagation of each eigenvector allows the distance between the sources to be determined (Fig. 21). Each pair of sources corresponds to one particular Lamb wave. At this frequency, the first and second eigenvectors are associated with the wave S_0, the third and fourth with the wave A_1 and the fifth and sixth with the wave A_0.
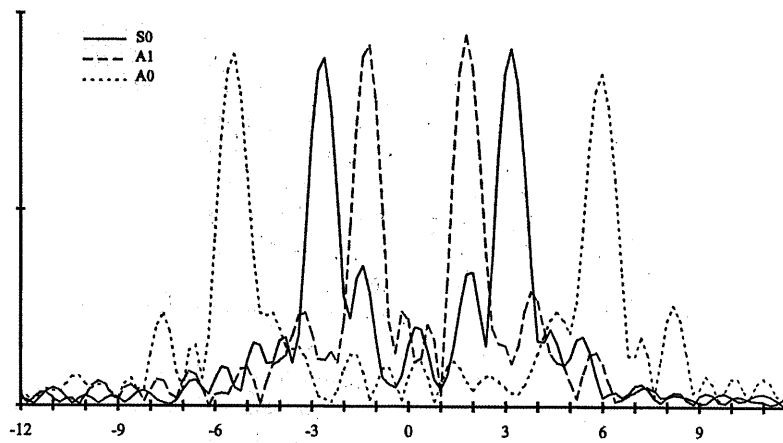

-12   -9   -6   -3   0   3   6   9

Fig. 21. Directivity patterns obtained by numerical propagation of eigenvectors 1, 3 and 5

The same calculation is done at several frequencies from 2.2 MHz to 4 MHz, so that the dispersion curves for the three waves can be plotted (Fig. 22). These curves are very close to the theoretical curves obtained for a steel plate of thickness of 0.6 mm. In particular, the determination of the cutoff frequency of the wave A_1 allows the thickness of the shell to be found.

One limitation of this method is that the generation points of the circumferential waves need to be spatially resolved. In the case of two waves of close phase velocities, the separation may not be possible. As the phase velocity increases, the two generation points get closer and are no longer resolved by the system. This partly explains the reason why the velocity of the wave A_1 could not be measured closer to the cutoff frequency.
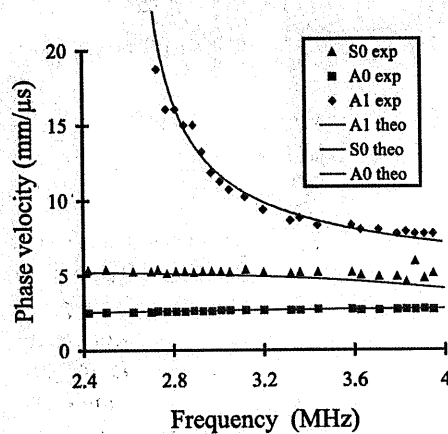

Fig. 22. Dispersion curves: theory and experiment

5.3   Resonance Frequencies of the Shell

The eigenvalue associated with one particular wave depends on the frequency; it is proportional to the level of contribution of the wave to the scattered field. Beside the reponses of the transducers, the generation and radiation coefficients of the wave are responsible for these variations. Moreover if the dynamics and duration of the recorded signals allow several turns of the wave around the shell to be detected, a fast modulation of the corresponding eigenvalue versus frequency is induced, the maxima corresponding to the resonance frequencies of the shell. In the experiment, the wave A_0 is attenuated so fast that only one turn can be observed. But several turns of A_1 and S_0 contribute to the scattered field. To take into account these multiple turns, the time-reversal operator was calculated using 40 ms of signal. Then the eigenvalues of the time-reversal operator were calculated from 2.2 MHz to 3.8 MHz. The first six eigenvalues are represented versus frequency in Fig. 23. The two
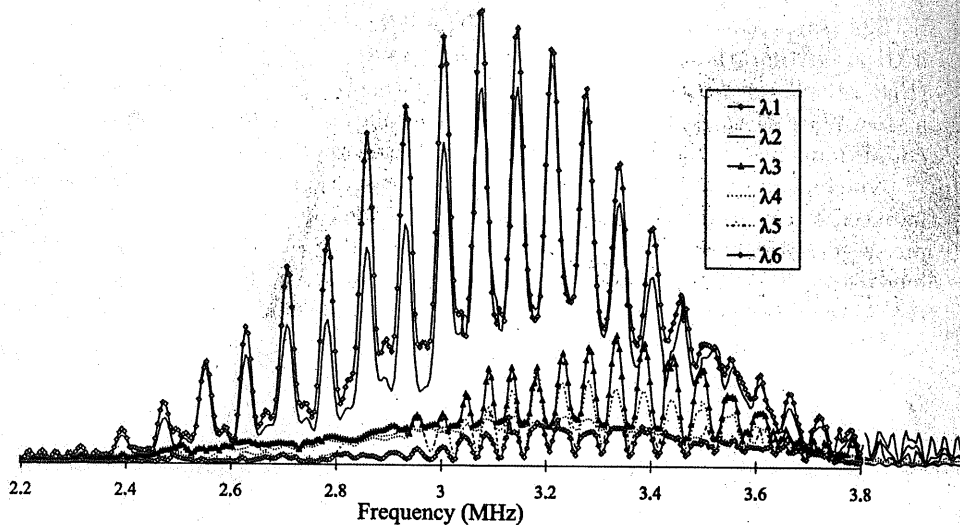
Fig. 23. Eigenvalues of the time-reversal operator versus frequency

curves $\lambda_1(\omega)$ and $\lambda_2(\omega)$ correspond to the wave S_0. Their maxima occur at the resonance frequencies of the shell corresponding to this wave. The width of the peaks is mainly due to the length and dynamic of the recorded signals, which allow only three turns of S_0 wave around the shell to be seen. Similar observations can be made for the wave A_1. This wave is associated with the eigenvalues $\lambda_3(\omega)$ and $\lambda_4(\omega)$ around their corresponding resonance frequencies and with $\lambda_5(\omega)$ and $\lambda_6(\omega)$ near their corresponding anti-resonance frequencies. The resonance peaks are well defined although the contribution of the wave A_1 is weaker than that of S_0.

The D.O.R.T method provides the resonance frequencies due to the waves S_0 and A_1, with the significant advantage that close resonance frequencies can be distinguished.

6   The D.O.R.T. Method in the Time Domain

In the preceding sections, analysis of the transfer function is done frequency by frequency. Only a small part of the information contained in the inter-element impulse response functions is used. In fact, the decomposition of the time-reversal operator can be done at any frequency. In order to get temporal signals, it would be natural to calculate the eigenvectors in the whole band of the transducers and to perform an inverse Fourier transform of the eigenvector function of the frequency. However, this operation is nontrivial. The main reason is that the scatterers' reflectivity generally depends on frequency, so that at one frequency the first eigenvector can be associated to one scatterer, while it is associated to another one at another frequency. However, if the

strengths of the scatterers are sufficiently different, then the first eigenvector may correspond to the same scatterer in the whole frequency band of the transducers. In this case, it is possible to build temporal signals from the eigenvectors. If the first eigenvector corresponds to one point-like scatterer, then the temporal signal will provide the impulse Green's function connecting the scatterer with the array.

6.1   Construction of the Temporal Green's Functions

The above-mentioned conditions are satisfied in the following example. The array of transducers and the waveguide are the same as in Sect. 1. The range of the scatterers is 400 mm, the distance between the scatterers is 2 mm, and their reflectivities differ by a factor of three in the frequency band of the transducers. The SVD of the transfer matrix is calculated at each frequency of the discrete spectrum from 0.8 to 2.2 MHz. The singular values, distribution versus frequency is shown Fig. 24: two singular values are apart from the 58 noise singular values and well separated from each other.

The impulse response function from the strong scatterer to the array can be reconstructed from the eigenvectors $\sqrt{\lambda_1(\omega)}V_1(\omega)$. Assuming the reflectivity of the scatterer is independent of the frequency, this response is the temporal Green's function connecting the scatterer to the array convoluted by the acousto-electrical response of the transducer (Fig. 25, top). The same procedure applied to $\sqrt{\lambda_2(\omega)}V_2(\omega)$ provides the impulse Green's function from the second scatterer to the array (Fig. 25, bottom). This result is of
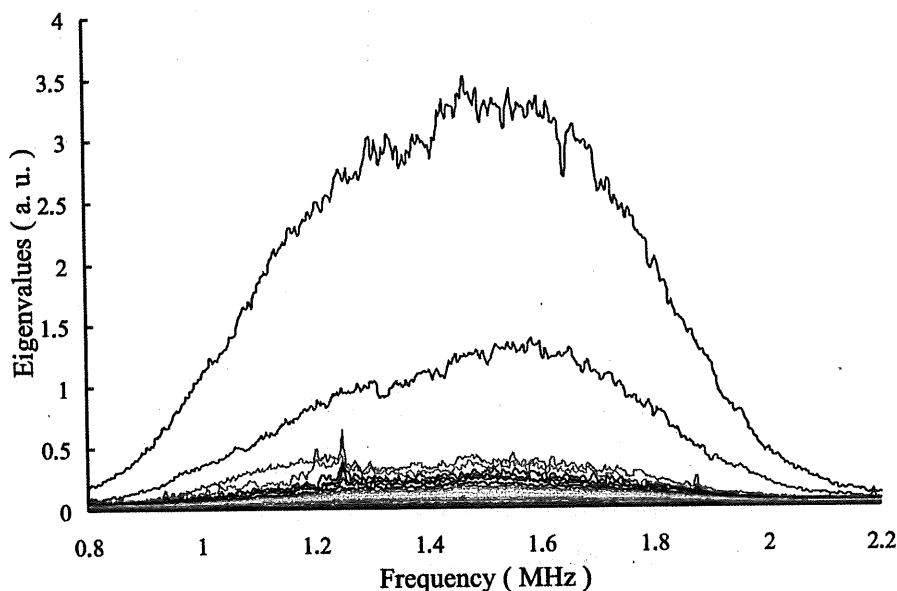

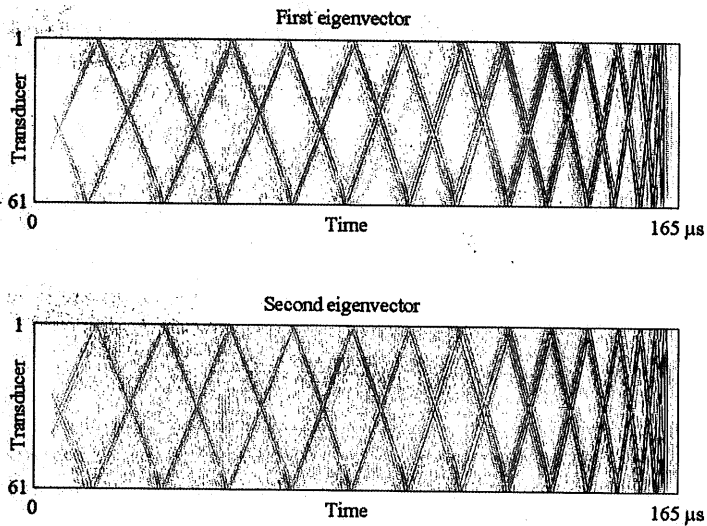Fig. 24. Singular values of the transfer matrix versus frequency

First eigenvector

Time   165 µs

Second eigenvector

Time   165 µs

Fig. 25. Signals reconstructed from (a) the first eigenvector and (b) the second eigenvector. These signals correspond to the impulse response from each wire to the array

particular interest in a complex propagating medium such as a waveguide. Indeed, the low signal-to-noise ratio due to the length of the multiple path and the complexity of the echographic response of scatterer due to the double paths along the guide render the determination of the impulse responses of the scatterers very difficult.
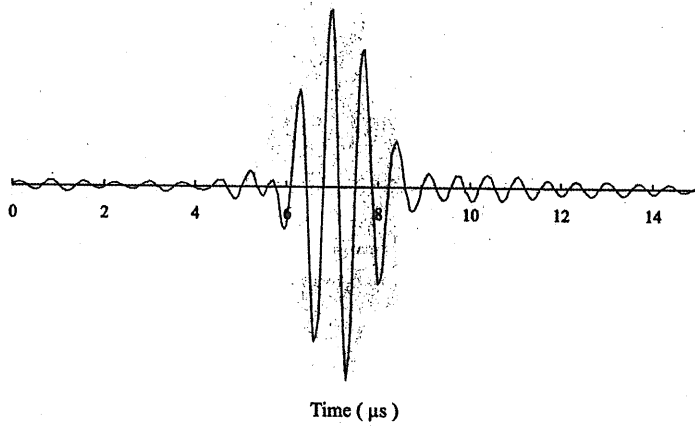

Time (µs)

Fig. 26. Time-domain compression: signal received at the position of the first wire after transmission of the first temporal eigenvector
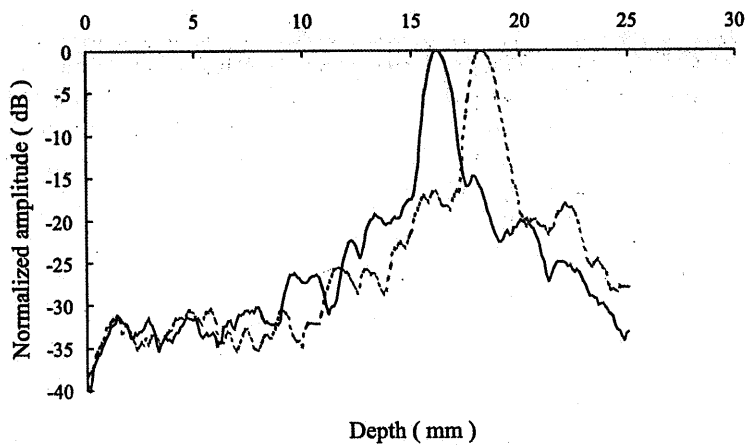
Fig. 27. Maximum of the pressure field measured at the depth of the wires across the guide after transmission of eigenvectors 1 and 2

6.2 Selective Focusing in the Pulse Mode

These signals are then transmitted from the array and the so-produced field is recorded along a line at the initial depth of the wires. One can observe an excellent temporal compression at the position of the wires: the signal received at the wire position is a pulse 3-ms long, while the transmitted signals are 165-ms long (Fig. 26).
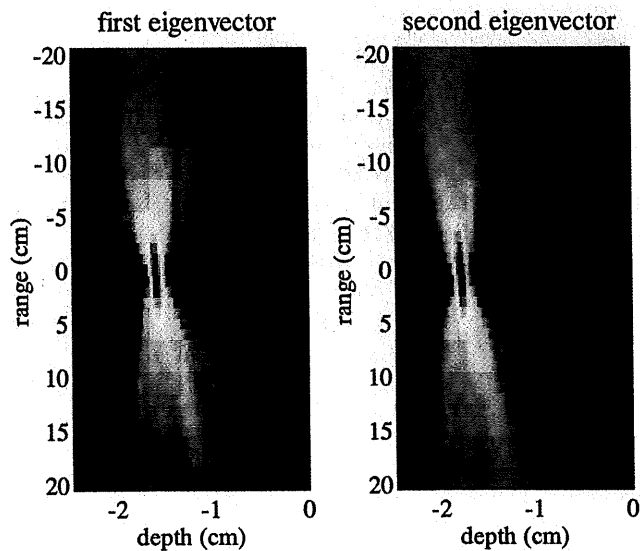

Fig. 28. Two-dimensional map of the maximum of the pressure field measured after transmission of the first and second eigenvectors

The transverse peak pressure pattern of the first and second eigenvectors at the depth of the wire (Fig. 27) can be compared with the one obtained in monochromatic transmission (Fig. 11). The improvement in spatial focusing is undeniable. The secondary lobes decrease to $-30\,\text{dB}$, while in the monochromatic transmission they remained around $-18\,\text{dB}$. Furthermore, the focusing is also excellent in range (Fig. 28)

7 Conclusion

In brief, the D.O.R.T. method is a generalization of the principle of iterative time-reversal mirrors. It allows the different waves contributing to the scattered field to be sorted and provides information on the scattering medium that up to now has not been available. It is a powerful tool for detection and focusing in heterogeneous and multiple target media and more generally for inverse scattering analysis.

The various experimental results shown opened several axies of research that are now under study. The detection of microcalcification in the breast is probably one of the most interesting applications in medical imaging. The D.O.R.T. method can be applied to nondestructive testing in solid waveguides. This is of particular interest for finding defects that are close to the interfaces. The results presented in a nonstationary guide are promising and have motivated further studies of underwater applications such as mine countermeasures. The time-domain D.O.R.T. method could be used in detection to reduce sidelobe effects such as problems of false location.

References

1. M. Fink, C. Prada, F. Wu, Self focusing in inhomogeneous media with time reversal acoustic mirrors, Proc. IEEE Ultrason. Symp. **2**, 681–686 (1989)
2. M. Fink, Time Reversal Mirrors, J. Phys. D **26**, 1333–1350 (1993)
3. C. Prada, J.-L. Thomas, M. Fink, The iterative time reversal process: analysis of the convergence, J. Acoust. Soc. Am. **97**, 62–71 (1995)
4. C. Prada, M. Fink, Eigenmodes of the time reversal operator: a solution to selective focusing in multiple target media, Wave Motion **20**, 151–163 (1994)
5. C. Prada, S. Manneville, D. Spoliansky, M. Fink, Decomposition of the time reversal operator: detection and selective focusing on two scatterers, J. Acoust. Soc. Am. **99**, 2067–2076 (1996)
6. C. Prada, M. Tanter, M. Fink, Flaw detection in solid with the D.O.R.T. method, Proc. IEEE Ultrason. Symp. **2**, 681–686 (1989)
7. G. Bienvenu, L. Kopp, Optimality of high resolution array processing using the eigensystem approach, IEEE Trans. Acoust. Speech Sig. Proc. **31** (1983)
8. R. O. Schmidt, Multiple Emitter Location and Signal Parameter Estimation, IEEE Trans. Ant. and Prop. **AP-34**, 276–281 (1986)
9. B. Baggeroer, W. A. Kuperman, P. N. Mikhalevsky, An overview of matched field methods in ocean acoustics, IEEE J. Ocean. Eng. **18**, 401–424 (1993)

10. Parvulescu, Matched – signal ('MESS') processing by the ocean, J. Acoust. Soc. Am. 98, 943–960 (1995)

11. C. S. Clay, Optimum time domain signal transmission and source location in a waveguide, J. Acoust. Soc. Am. 81, 660–664 (1987)

12. S. Li, C. S. Clay, Optimum time domain signal transmission and source location in a waveguide: Experiments in an ideal wedge waveguide, J. Acoust. Soc. Am. 82, 1409–1417 (1987)

13. D. R. Jackson, D. R. Dowling, Phase conjugation in underwater acoustics, J. Acoust. Soc. Am. 89, 171–181 (1991)

14. P. Roux, B. Roman, M. Fink, Time-reversal in an ultrasonic waveguide, Appl. Phys. Lett. 70, 1811–1813 (1997)

15. W. A. Kuperman, W. S. Hodgkiss, H. C. Song, T. Akal, C. Ferla, D. R. Jackson, Phase conjugation in the ocean: Experimental demonstration of an acoustic time-reversal mirror, J. Acoust. Soc. Am. 103, 25–40 (1998)

16. H. C. Song, W. A. Kuperman, W. S. Hodgkiss, Iterative time reversal in the ocean, J. Acoust. Soc. Am. 105, 3176–3184 (1999)

17. W. S. Hodgkiss, H. C. Song, W. A. Kuperman, A long-range and variable focus phase-conjugation experiment in shallow water, J. Acoust. Soc. Am. 105, 1597–1602 (1999)

18. N. Mordant, C. Prada, M. Fink, Highly resolved detection and selective focusing in a waveguide using the D.O.R.T. method, J. Acoust. Soc. Am. 105, 2634–2642 (1999)

19. J.-L. Thomas, P. Roux, M. Fink, Inverse scattering analysis with an acoustic time-reversal mirror, Phys. Rev. Lett. 72, 637–640 (1994)

20. C. Prada, J.-L. Thomas, P. Roux, M. Fink, Acoustic time reversal and inverse scattering, Proc. Int. Symp. Inv. Prob. (1994) 309–316

21. C. Prada, M. Fink, Separation of interfering acoustic scattered signals using the invariant of the time-reversal operator. Application to Lamb waves characterization, J. Acoust. Soc. Am. 104, 801–807 (1998)